

Received March 26, 2018, accepted April 18, 2018. Date of publication xxxx 00, 0000, date of current version xxxx 00, 0000.

Digital Object Identifier 10.1109/ACCESS.2018.2829351

# Active Soft End Effectors for Efficient Grasping and Safe Handling

ALAA AL-IBADI<sup>1,2</sup>, (Member, IEEE), SAMIA NEFTI-MEZIANI<sup>1</sup>, AND STEVE DAVIS<sup>1</sup>

<sup>1</sup>School of Computing, Science and Engineering, University of Salford, Salford M5 4WT, U.K.

<sup>2</sup>Computer Engineering Department, Engineering College, University of Basrah, Basrah 61004, Iraq

Corresponding author: Alaa Al-Ibadi (alaa.falah77@yahoo.fr)

This work was supported by the Ministry of Higher Education in Iraq. The work of A. Al-Ibadi was supported by the Computer Engineering Department, University of Basrah.

**ABSTRACT** The end effector is a major part of a robot system and it defines the task the robot can perform. However, typically, a gripper is suited to grasping only a single or relatively small number of different objects. Dexterous grippers offer greater grasping ability but they are often very expensive, difficult to control and are insufficiently robust for industrial operation. This paper explores the principles of soft robotics and the design of low-cost grippers able to grasp a broad range of objects without the need for complex control schemes. Two different soft end effectors have been designed and built and their physical structure, characteristics, and operational performances have been analyzed. The soft grippers deform and conform to the object being grasped, meaning they are simple to control and minimal grasp planning is required. The soft nature of the grippers also makes them better suited to handling fragile and delicate objects than a traditional rigid gripper.

**INDEX TERMS** Soft robotics, pneumatic muscle actuators (PMA), self-bending contraction actuator (SBCA), circular pneumatic muscle actuator (CPMA), soft grippers.

## I. INTRODUCTION

Over recent years, several factors have driven researchers in both industry and academia to develop new grippers and robot end effectors. These factors include the need to decrease the cost of the systems and increase the range of products and materials a gripper can handle as robots are used in sectors other than traditional manufacturing [1]. When the human hand grips an object, the grasp is determined based on expectations of the object's weight and using feedback from the fingertips to prevent the object slipping by adjusting the grasp force [2]. In contrast, a typical mechanical robot gripper applies a fixed high force to the object to avoid slipping. This is inefficient in terms of energy use as often the grasp is firmer than is required and can also lead to damage if the object to be grasped is fragile. Similar techniques to that used by the human hand can be used in robots by attaching slip sensors to the robot gripper. The feedback from the tactile sensors reduces the experience reliability on robot operators and improves the end effector performance [2], [3].

The cost of a gripper can represent more than 20% of the cost of the whole robot system and is subject to the task requirements and the complexity of the part to be handled. It may also add additional complexity to the control system [4]. Typical traditional robot grippers were designed for

predefined jobs and could not be used for different object dimensions, weights or shapes other than where variations were small. If a system is to be re-tasked to handle different objects, this can require modification of, or indeed entire replacement of, the gripper. Various dexterous or multi-use gripper designs have been proposed to overcome this issue. However, the high cost of such types of grippers and maintenance problems make its use limited to a few applications [3], [4].

While the cost is considered a minor issue for some industrial applications, innovative new actuators, such as pneumatic muscle actuators (PMA), which are low cost, low weight, flexible and soft (in addition to the many other advantages), make it a potential alternative to previous robot end effectors. From this biologically inspired artificial muscle, human-like robot hands have been created with both industrial and medical applications [5].

A range of various actuated methods is recently used to design the soft robot grippers. Among these designs, Hassan *et al.* [6] and Rateni *et al.* [7] proposed a tendon-actuated soft three-fingers gripper made by using soft deformable materials. Giannaccini *et al.* [8] proposed tendons soft gripper to deform and move a fluid-filled soft deformable container. Katzschmann *et al.* [9] and Mosadegh *et al.* [10]

presented soft continuum fingers made as two different extensible layers to establish a bending behaviour. A multiple bending directions micro gripper is developed by Wakimoto *et al.* [11], the actuators bend according to the pressurised internal chambers. A very different structure of continuum soft hand was presented by Niiyama *et al.* [12]. The gripper uses recently developed hinged pouch motors, which when pressurized bending in joints. Generally, these types of grippers are not able to vary their stiffness. While extremely compliant fingers may be required for grasping some objects. Stilli *et al.* [13] and Maghooa *et al.* [14]. Al Abeach *et al.* [15] designed a variable stiffness gripper by varying a pressure inside the soft fingers which are made by an extension actuator and the grasping is occurred by tendons powered by contraction PMA.

Other types of soft grippers have been designed to provide compliant and safe grasping. The RBO hand by Deimel and Brock [16] provides compliance which allows the hand to face its surfaces to that of an object in response to contact forces. Due to the softness, the RBO offers shape matching to increment the contact surface between hand and object without the requirement for obvious sensing and control. The hand's fingers are based on similar principles to that of the PneuNet actuator [17]. The grasping force for this hand is up to 0.5 kg for three fingers. Deimel and Brock [18] present the RBO hand-2, which is made similar to the human hand of five fingers. The weight of this hand is 178 g and it can grasp objects up to 0.5 kg. A three finger soft hand is designed by Homberg, *et al.* [19] which is able to grasp a range of objects and can be mounted on existing robots used for grasping.

Several soft grippers have been presented in terms of safe grasping, among them, Amend *et al.* [20] presented different commercial sizes of vacuum soft grippers varying from 1 mm to 1 m in diameter and able to grasp up to 3 kg, while, the gripper weight is varying from 1.1 kg to 2.9 kg. Wang *et al.* [21], Nordin *et al.* [22] and Faudzi *et al.* [23] developed a bending actuator by using different braided angles and this idea has been used by Wang *et al.* [24] to design a two-finger gripper to grasp an object by bending around it. the maximum experimental grasping force for their gripper is 61 g. Guo *et al.* [25] presented a stretchable electroadhesion soft gripper by using a combination of the electrostatic force and a pneu-net [10] soft bending actuator. Shintake *et al.* [26] designed an electrostatically actuated bending soft gripper able to grasp different object shapes.

Numerous research have been done to develop a bending soft actuator. Among them, Razif *et al.* [27] presented a bending actuator by controlling the air pressure in two chambers and it is analyzed by Razif *et al.* [28]. Natarajan *et al.* [29] design a soft robot finger has the ability to form in different bending directions according to the coverage mesh shapes.

In this article, contraction and the extension PMAs are used to design two-end effectors. A self-bending contraction actuator (SBCA) is presented and its structure and performances are explained. A three-fingers gripper has been designed based on SBCA presented and its characteristics have been

illustrated. Moreover, another three fingers are added to build a six-fingers gripper of two layers of contact points to increase the grasping performance. A novel design of the circular pneumatic muscle actuator (CPMA) is proposed. The novel CPMA is inspired by human facial muscles and it is used with an extensor pneumatic muscle actuator to design an extensor-circular gripper, which provides an extraordinary grasping force in comparison to its weight, and then the design is developed by increasing the number of CPMAs to three. The modified design provides an extremely strong force able to grasp an object weighing up to 40 kg. The proposed new grippers are built to adapt to the shape of the object being grasped, allowing many different shaped objects to be grasped with a single device. They also seek to enhance efficiency by increasing the amount of payload that can be grasped whilst minimising power requirements and decreasing the control complexity when grasping objects.

The main contributions of this article are modifying the McKibben contraction actuator to establish a bending performance, and then design two grippers according to the presented modification. The second novelty is using the fact of the circular "Orbicularis Oculi" human facial muscle which controls the movements of both the mouth and the eyes to design a circular pneumatic muscle actuator and use it with the extensor actuator to design a high grasping force gripper.

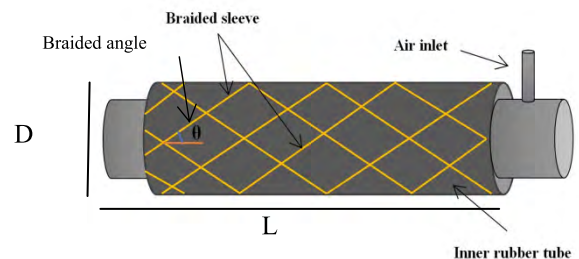
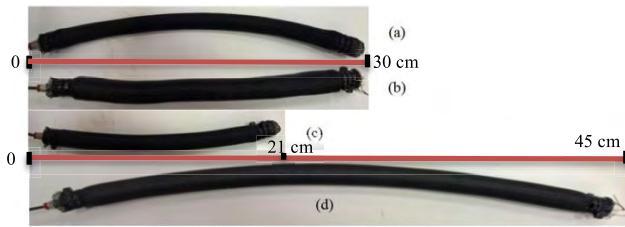


FIGURE 1. The structure of the pneumatic muscle.

## II. THE PNEUMATIC MUSCLE ACTUATOR

The PMA can be classified as a contractor or extensor actuator depending on the construction. Fig. 1 shows the simple structure of the PMA. The initial values of both the length ( $L$ ) and the diameter ( $D$ ) can be defined as ( $L_0$  and  $D_0$ ), respectively; these values are subject to the length and diameter of both the inner tube and the braided sleeve. The resting unpressurised value of the braided angle ( $\theta$ ) determines whether the muscle will extend or contract when pressurised. The muscle will be a contractor PMA if  $\theta$  is less than  $54.7^\circ$  and an extensor PMA if the resting braid angle is greater than  $54.7^\circ$  [30]–[32].

Sárosi *et al.* [33] argue that the maximum contraction ratio for the contractor actuator is 25%, though it depends on the structure of the PMA, the stiffness and diameter of the inner rubber tube [34], in addition to the maximum diameter of the braided sleeve, but it cannot be more than 35% [30], [35]. On the other hand, the extensor PMA could be extended by up



**FIGURE 2.** Two 30 cm PMAs at different pressurised conditions, (a) is the contractor actuator at zero pressure (b) is the extensor actuator at zero pressure (c) is the contractor actuator at 400 kPa and (d) is the extensor actuator at 400 kPa.

to 50% [36], [37]. Equation (1) defines the contraction ratio and (2) describes the extension ratio, respectively.

$$\varepsilon = \frac{L_0 - L}{L_0} \quad (1)$$

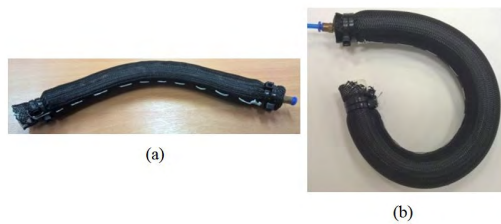
$$\dot{\varepsilon} = \frac{L - L_0}{L_0} \quad (2)$$

Fig. 2 shows the effect of the pressure on both the contractor and the extensor actuators.

McMahan *et al.* [36] explain that using the principle of constant-volume creates the bending behaviour of the extensor PMA, where the dimensional adjustment on one side leads to a dimensional modification on another side.

The traditional way in which PMAs are used is to produce a linear contraction or extension. However, this research explores using the actuators in such a manner that when activated, they bend.

To achieve the bending behaviour for the extension PMA, a thread is used to fix one side of the actuator, which prevents it from extending, while the other side is free to elongate. The whole muscle will bend toward the thread side when pressurised. Fig. 3 shows a 30 cm extensor actuator and how it bends when supplied with 300 kPa pressure.



**FIGURE 3.** A 30 cm extensor PMA (a) one side sewed actuator (b) under 300 kPa air pressure.

Bending can also be achieved by connecting multiple extensor actuators in parallel and fixing them together along their entire length to form a continuum arm [38]. Fig.4.a illustrates an extensor continuum arm, which is constructed from four 30 cm actuators.

The pressure is increased with one of the PMAs in the corner. The arm will then bend into another position depending on the amount of P in the muscle and the attached load. The maximum angle at no load in the test continuum arm was

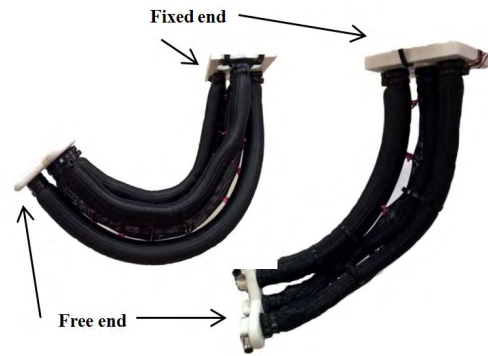


**FIGURE 4.** The continuum arms at 300kPa. (Left) An extensor arm, (Right) a contractor arm.

measured at 164°, while it is reduced to 116° at a 0.5 kg payload.

A contractor PMA cannot be made to bend by using the thread as in Fig.3 because the actuator length decreases during its operation and the thread is unable to resist this. However, bending can be achieved using contractor muscles if they are formed into a continuum arm. Al-Ibadi *et al.* [35] demonstrated a continuum arm that uses 4-PMAs as shown in Fig.4.b. The authors explain that the maximum angle without load was found to be 84° and this angle reduced to 47° when the attached load increased to 0.5 kg.

A contractor PMA has a higher force output than an extensor of the same dimension, so there is an advantage to using a contractor muscle. However, as has been shown above, to generate a bending motion using contractor muscles, multiple actuators must be used in a continuum like structure.

The problem is that increasing the number of actuators increases the complexity of the control system and hardware needed. The only way to make a single actuator bend is by fixing one side to prevent it from changing length. For the contraction actuator, a thin (2 mm) flexible but incompressible reinforcing rod is made by 3D printing, as shown in Fig. 5.

It has been placed between the inner rubber tube and the braided sleeve for the 30 cm contraction actuator and sewed to the sleeve to fix its position. Fig. 6 shows a bent PMA at 300 kPa.

Experiments have been performed to study the bending angle of the proposed actuator at different values of the attached load by applying an air pressure through a (3/3 Matrix) solenoid valve and read the bending angle by MPU 6050 sensor via Arduino Mega 2560. Table 1 lists the maximum bending angle at various loads.

### III. THREE FINGERS GRIPPER BASE ON SELF-BENDING CONTRACTION PMA

The proposed bending contractor actuator has been used to build a three finger gripper as shown in Fig. 7. Three identical actuators of 14 cm resting length were constructed using a 14 cm thin reinforcing rod placed along one side.

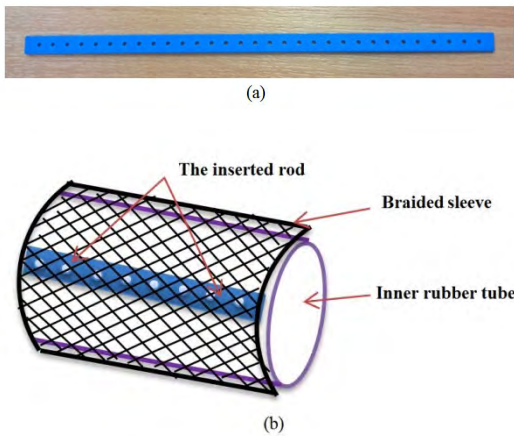


FIGURE 5. A novel contractor PMA. (a) A 3D printed thin incompressible reinforcing rod, (b) Explain the inserted rod.

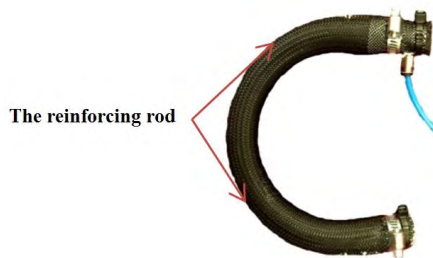


FIGURE 6. A 30 cm self-bending contraction PMA.

TABLE 1. The maximum bending angle at different loads.

Load (kg)	Bending angle (degree)
0.0	213.1
0.5	136.2
1.0	73.0
1.5	49.3
2.0	34.1

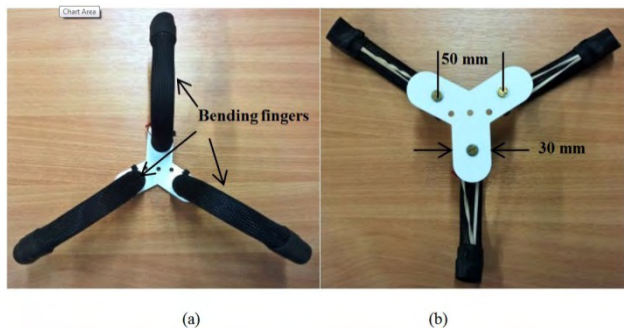


FIGURE 7. A three finger gripper based on self-bending contraction PMA.

To maximize the range of motion in the fingers, a thin ribbon of elastomeric material is placed on the rear of each finger which causes the fingers to spread when the actuator is unpressurised. The top base of the gripper is made by a 3D printer and the complete gripper is shown in Fig. 7.

The presented gripper can spread its fingers so that they are at a maximum of 20 cm apart and close them to the point where all fingers touch each other. This allows the gripper to grasp a large range of different object sizes.

In addition to the other advantages of the PMA, the proposed gripper has more benefits than other grippers for numerous reasons, such as low cost, which is about 10 dollars, easy to manufacture, wide dimension grasping ability, safe to low stiffness objects and it has a low mass (0.18 kg). Its inertia is also low, which potentially makes it safer for operation around humans.

In addition, it is easy to control by adjusting the air pressure in all fingers simultaneously, and the closed loop control is not needed to ensure that the three fingers make contact with the object because the fingers are compliant and will automatically bend around objects. To do this with a rigid noncompliant hand would require grasp planning and precise control of each finger.

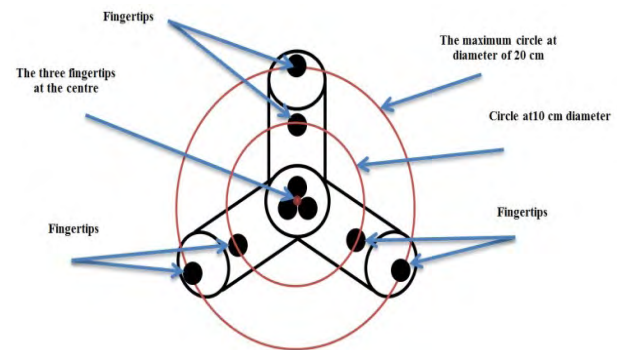


FIGURE 8. The fingertips of the gripper at different positions.

Fig. 8 shows that for cylindrical objects, the fingertips form a circle shape at different diameters, which depends on the diameter of the object.

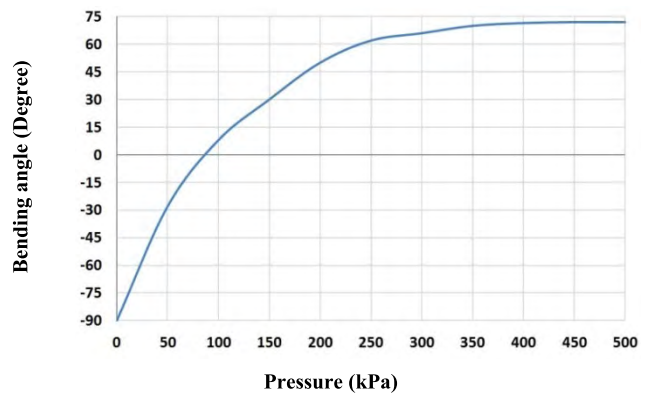


FIGURE 9. The bending angle -pressure characteristics for each finger.

Fig. 8 shows that for cylindrical objects, the fingertips form a circle shape at different diameters, which depends on the diameter of the object. While different object shapes lead to putting the fingertips at different positions. The bending angle of the proposed fingers is illustrated in Fig. 9. This

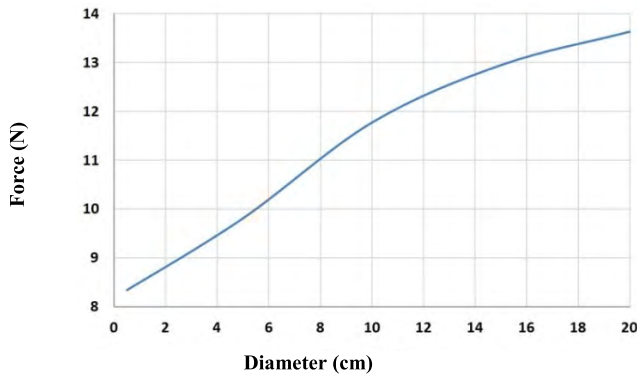


FIGURE 10. The force of a single finger at different positions.

figure shows that the maximum bending angle for each finger is  $72^\circ$ , which is more than is required to put them together at the centre of the gripper. Therefore, the force can be adjusted to grasp small objects such as the pen in Fig. 12.

Fig. 10 shows that the force of a single finger is high at large cylinder diameters and decreases for smaller sizes. Because the finger’s pressure for the small diameter is higher than the pressure for the big size, the pressure difference from the touch point to the maximum value (500 kPa) is reduced when the diameter is decreased since the finger needs more pressure to bend more. That reduces the force applied by the finger. Table 2 lists the minimum air pressure required to touch different diameter objects.

TABLE 2. The maximum bending angle at different loads.

Object diameter (cm)	Minimum required pressure (kPa)
0.5	126
5	110
10	76
15	55
20	47

The maximum force for each finger is found at different bending angles, as follows:

- Cylindrical objects of different diameters are used for grasping by the proposed gripper.
- A force sensor is fixed at the fingertip to find the force value at each position.
- The pressure is increased manually from zero to the point of the force sensor start reading. This pressure has been recorded, by a pressure sensor, as a minimum required pressure to touch the object.
- The pressure then increases until it reaches the 500 kPa. At this point, the maximum force value is recorded.
- Fig. 11 shows the maximum force of each finger at different diameters.

An experiment was undertaken to discover the maximum gripper payload with a 6 cm diameter cylindrical object of different weights. At each load value, the pressure was applied until the grasping operation occurred without slipping,

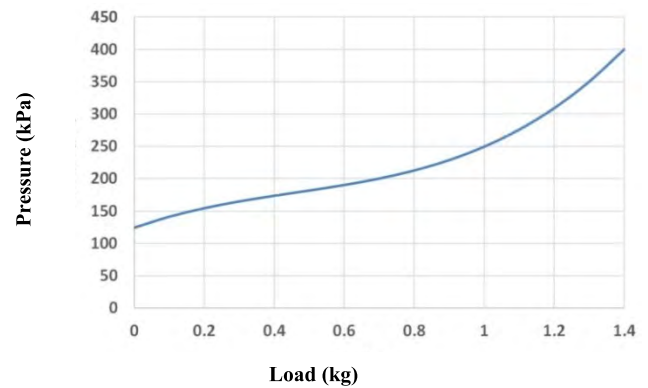


FIGURE 11. The payload–pressure characteristics for the three-fingers gripper.

then the experiment was repeated and the corresponding air pressure amount recorded. As a result, the payload for this gripper at this specific diameter is 1.4 kg but the grasping payload differs depending on the object’s dimensions, as shown in Fig. 10. The experiment results are illustrated in Fig. 11, which shows that the grasping force is increased by applying more pressure to the fingers. The presented gripper has an advantage over the designed gripper in [16], [18], and [19] due to its increased grasping load. While the proposed gripper has a similar weight to the RBO hand and RBO hand 2, it provides an about three times of grasping weight.

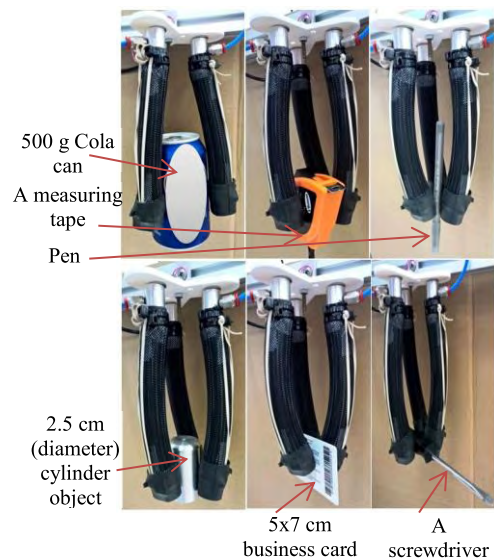


FIGURE 12. Multiple objects grasped by the proposed gripper.

Different object shapes could be grasped as shown in Fig. 12. The pressure required to ensure contact between the fingertips when grasping depends on the dimensions of the target objects. However, the force needed can be defined as:

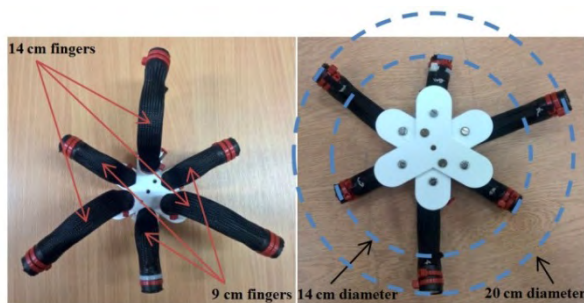
$$F = \frac{m(g + a)}{\mu n} \times s \tag{3}$$

Where  $F$  is the required grasping force in (N),  $m$  works part weight (kg),  $g$  is the gravitation acceleration and is

approximately equal to  $9.81 \text{ (m/s}^2\text{)}$ ,  $a$  is the acceleration of movement,  $\mu$  is the friction coefficient and is dependent on the material of both the finger and the object,  $n$  represents the number of fingers and is equal to 3 in this case, and  $s$  is the safety factor.

**IV. INCREMENT OF GRASPING POINTS**

To increase the grasping force of the proposed gripper, three more fingers are added to the design but the finger lengths are less. This modification provides six grasping points of two groups of three. The length of the long fingers is 14 cm, while the length of the others is 9 cm. Therefore, the objects will be grasped by six points as shown in Fig. 13.



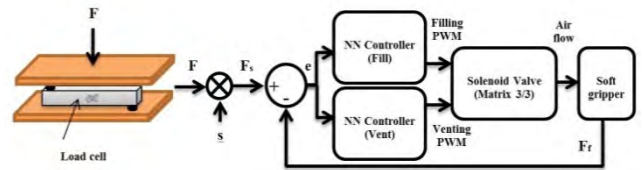
**FIGURE 13.** The layout of the six bending fingers.

Fig. 13 illustrates that the long fingers grasp an object of up to 20 cm in dimension and the small group can start grasping from 14 cm. A similar experiment for the three finger gripper was also done to find the maximum grasping payload for cylindrical objects of 14 cm diameter, which represents shapes of the maximum dimension to be grasped by the six fingers. The results show that the maximum grasping payload is 3.6 kg and the maximum bending angle of the small finger is  $26^\circ$ . The weight of the new gripper is 0.34 kg, while it provides 2.57 times of the previous gripper, which represents 7.2 times that of RBO hands.

**V. THE GRASPING CONTROL OF DIFFERENT LOADS**

The grasping control of different objects is a challenge for this type of soft gripper. In this section, a neural network (NN) controller has been designed using Matlab to control the required grasping force according to the weight of the object. The NARMA-L2 NN-controller is used of 9-neurons in one hidden layer, 3-delayed plant inputs, 2-delayed plants outputs and it is trained by (trainlm) for 100 Epochs. The mean square error (MSE) for the training, testing and validating data is about  $10^{-7}$ . Fig. 14 shows the block diagram of the control system.

In this control system, a 10 kg load cell has been used and the weight scale is designed as shown in Fig. 14. The designed weight scale is used as a base for the object and it provides the force ( $F$ ) to the controller via Arduino Mega 2560 and multiplies it by a safety factor ( $s$ ); the resulting force is a set point ( $F_s$ ). While the feedback force ( $F_f$ ) is provided by a



**FIGURE 14.** The full block diagram of the grasping force control system.

force sensitive resistance (FSR-402), which is mounted on the fingertip of one finger, the diameter of the active area for this sensor is 12.5 mm and the output force is multiplied by 3 to give the sum of the force of the gripper. According to the error sign between  $F_s$  and  $F_f$ , the controller will activate either the filling part or the venting part by sending the appropriate duty cycle of the pulse width modulation (PWM) to control the solenoid valve.

An approximate relationship between the force and the duty cycle is used to train the NN controller as:

$$y = \frac{17.85 \times u}{98} \tag{4}$$

Where  $y$  is the gripper force in (N), the number “17.85” represents the maximum force produced from the gripper in (N),  $u$  is the controlled duty cycle and the “98” refers to 98% of the maximum duty cycle for the control signal to avoid the continued supply to the solenoid valve. The controller is validated by applying sinusoidal and step set signals at 0.25 and 0.5 Hz as shown in Fig. 15.

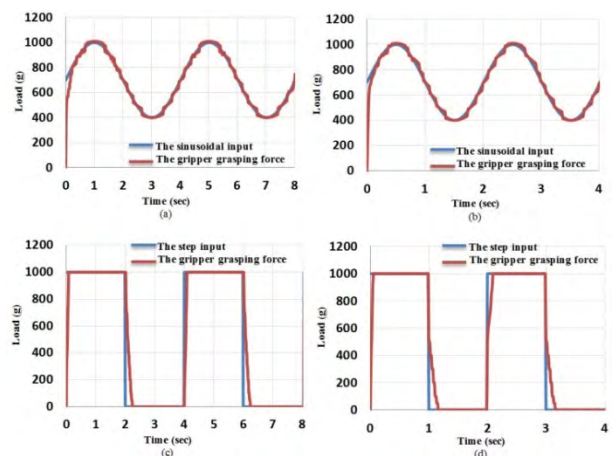


**FIGURE 15.** The controller response for the three finger gripper. (a) The sinusoidal response at 0.25 Hz, (b) The sinusoidal response at 0.5 Hz, (c) The step response at 0.25 Hz and (d) The step response at 0.5 Hz.

Fig. 15 illustrates that the controller is accurate enough to be used for different object weights. The sinusoidal response shows that the signal of the force sensor tries to track the input signal with a constant error due to the continuous changing.

Moreover, the step response has a zero steady state error because of its constant values at zero and 1000 g.

On the other hand, the time of release is higher than at the time of grasping because the time of grasping because the

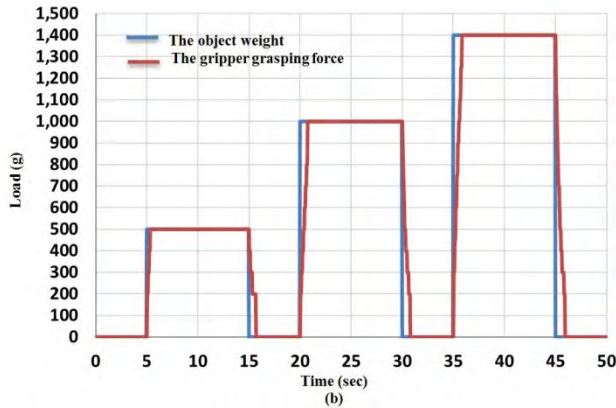
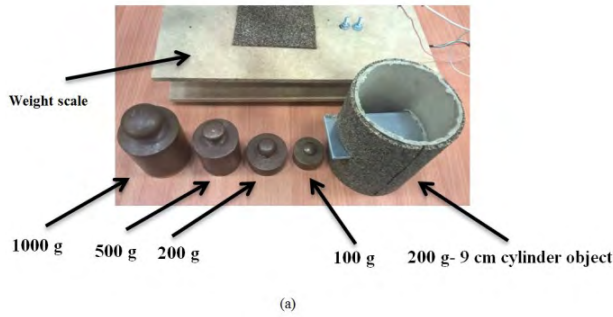


FIGURE 16. The grasping force control. (a) The weight scale and the object. (b) The response of the gripper due to different load values.

time needed to vent the muscle is more than the time needed to fill it. This occurs for two reasons: the hysteresis of the PMA and the difference between the air pressure inside the actuator and the outside air pressure.

To examine the effectiveness of the proposed gripper and the control system, an adjustable weight cylinder object is used for three different load values (500 g, 1000 g and 1400 g). Fig. 16 shows the object and the control performance.

Fig. 16.b shows that the steady-state error is zero for different load values. The maximum pressure for this process is 110 kPa, 240 kPa and 390 kPa for the object loads 500 g, 1000 g and 1400 g, respectively. Moreover, the safety factor is set to 1.3 to prevent slipping during the grasping process.

## VI. EXTENSION-CIRCULAR GRIPPER

Human facial muscles have unique features. They lie on the top of the body joints and their function is either to open and close the orifices of the face or to pull the skin into intricate actions, creating facial expressions. The circular “Orbicularis Oculi” muscle controls the movements of both the mouth and the eyes. The contraction of this muscle decreases the mouth slot, while the resting causes the mouth to open. Similar effects occur in the human eyes [39].

This singular type of human skeletal muscle inspired us to design the CPMA, which has an ability to decrease its inner area by shrinking the outer and inner circumference and increase its diameter.

The way to build a contraction PMA is also used to design and implement the CPMA. Similar lengths of a braided sleeve of 1.2 to 3 cm diameter variation and a rubber tube of 1.1 cm diameter are used to build the CPMA. The two ends are connected together by a 5 cm aluminium cylinder.

By pressurising the actuator, both the outer and the inner diameter of the CPMA will reduce, while the diameter of the actuator itself will increase until the braided angle reaches its critical value or the maximum value of the sleeve diameter is achieved. The triple diameter changes lead to a decrease in the opening area.

The opening area at relaxed conditions (zero air pressure) depends on the rest length of the braided sleeve and its diameter.



FIGURE 17. The structure of the extension-circular gripper.

A novel soft gripper is proposed in this section by using the extensor and the CPMA. Fig. 17 explains the structure of this gripper, which is built using three 18 cm extensor actuators and one CPMA.

The extensor actuators provide an ability to extend and bend in addition to increasing the gripper’s stability, while the grasping occurs due to the circular actuator, which is made as a 30 cm simple contractor muscle. The maximum inner diameter for the gripper is 7.8 cm.

Experiments have been done to define the performance of the proposed gripper. Air pressure is applied by using a solenoid valve to the extensor actuators, which changes the length of the gripper. The length of the gripper changes with pressure until it reaches the maximum length of 24 cm at 500 kPa with an extension ratio of 33%. Then pressure is applied to the CPMA and the inner diameter is reduced to the minimum of 4.45 cm at 400 kPa. Fig. 18 shows the diameter and the length as a function of pressure. Further air pressure is added to the CPMA but the inner diameter remains constant because the contractor muscle reaches its maximum contraction ratio so that the percentage of the diameter reduction after the 400 kPa can be ignored.

The diameter reduction ratio (DRR) can be calculated from (5) and it is equal to 43% for the presented gripper.

$$DRR = \frac{D_0 - D}{D_0} \quad (5)$$

Where:  $D_0$  is the diameter at zero pressure and  $D$  is the diameter at pressurised condition.

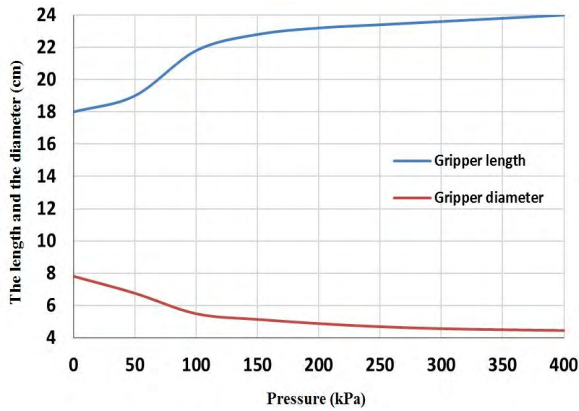


FIGURE 18. Variation of the length and the diameter for the extension-circular gripper.

The extension-circular gripper has an advantage over multi-finger grippers due to an infinite number of contact points between the inner surface of the CPMA and the object to be handled. This preference increases the applied force and provides a significant grasping stability. On the other hand, pressurising the extensor PMAs simultaneously results in increasing the gripper length, as shown in Fig.18, while different pressure amounts in each actuator lead to moving the circular actuator in multiple directions. The maximum angle is 61° in relation to its original position and can be achieved by applying air pressure to one actuator. These performances increase the efficiency of the gripper by adding the bending behaviour.

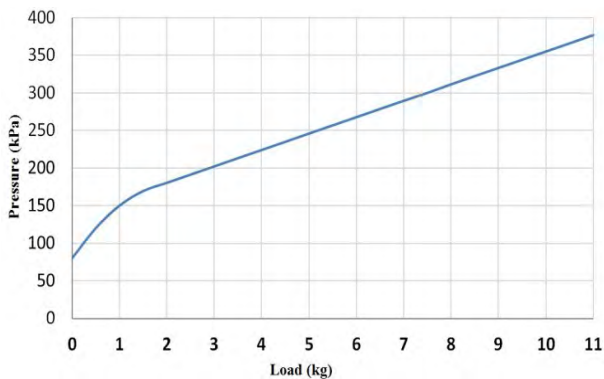


FIGURE 19. The payload –pressure characteristics for the extension-circular gripper.

To explain the pressure-payload characteristic for this gripper, an experiment has been done by selecting multi-weight cylindrical objects of 6 cm diameter. The load starts at 0.5 kg and is then increased by 0.5 kg steps. At each step, the applied air pressure is raised to prevent slipping. Fig. 19 illustrates the experimental results and shows that the maximum payload for the presented gripper is 10.9 kg for the 6 cm object and the payload–pressure characteristic is linear above the 1.5 kg load. The parameter to be controlled for the extension-circular gripper is the air pressure in the circular actuator, which provides an easy strategy for achieving the grasping operation.



FIGURE 20. Multiple objects grasped by the extension-circular gripper.

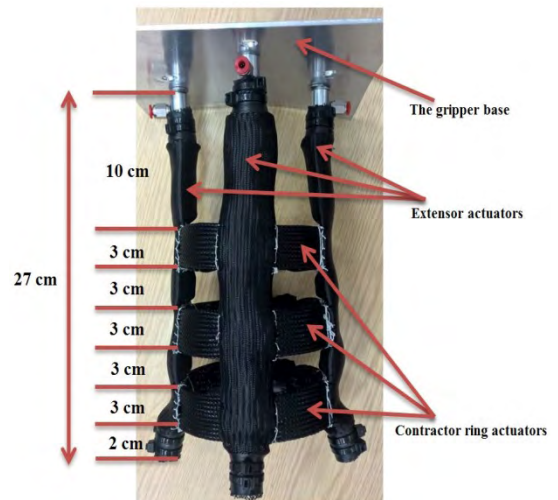


FIGURE 21. The dimensions and the structure of the three CPMA's gripper.

Objects of various shapes can be grasped; however, their size has to be limited to no more than 3.9 cm between the object's centre and its edge. Fig. 20 shows the grasping of different object shapes and weights require different grasping force; however, the proposed gripper provides equal grasping force for all contact points between the objects and the CPMA. The direction of these forces is toward the centre of the circle.

**VII. THREE CPMA'S GRIPPER**

In this section the extensor-circular gripper is redesigned by increasing the number of CPMA's to three so as to increase the grasping payload. In this design, the length of the gripper at zero pressure is 27 cm and it is increased to 38.1 cm

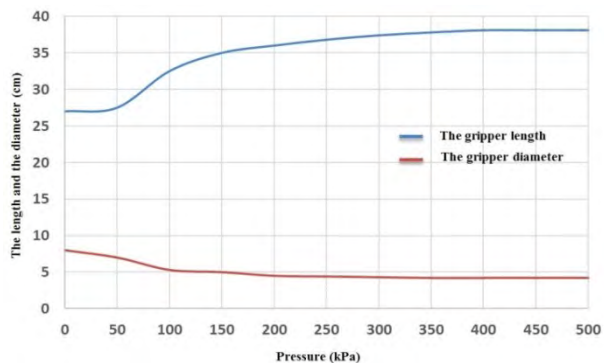


FIGURE 22. Variation of the length and the diameter for the three CPMS gripper.

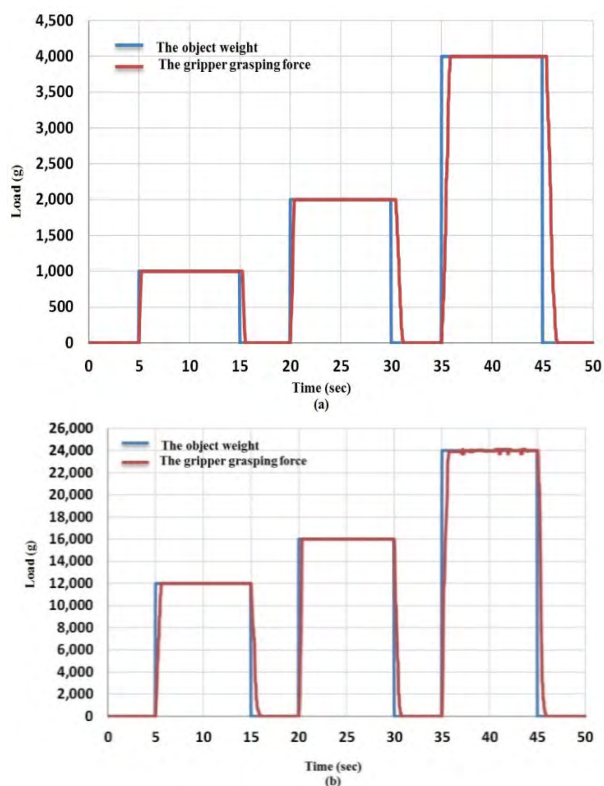


FIGURE 23. The grasping force control. (a) The grasping control results for the one CPMA gripper at three different loads (b) The grasping control results for the three CPMA gripper at three different loads.

at 500 kPa. From (2) the extension ratio for the extensor muscles is 41%. The diameter for each CPMA is from 8 cm to 4.3 cm for the maximum pressure of 400 kPa. The diameter reduction ratio for these circular actuators is 46%.

Fig. 21 illustrates the three CPMA gripper and its performances are illustrated in Fig. 22.

A similar experiment in section VI is used to define the grasping load of the three CPMA gripper. For a cylindrical object with a 6 cm diameter the gripper can grasp up to 40 kg while it weight is 0.8 kg.

VIII. THE CONTROL SYSTEM OF THE CPMA GRIPPER

A similar control system for the finger gripper is used in this section but we changed the load cell maximum load

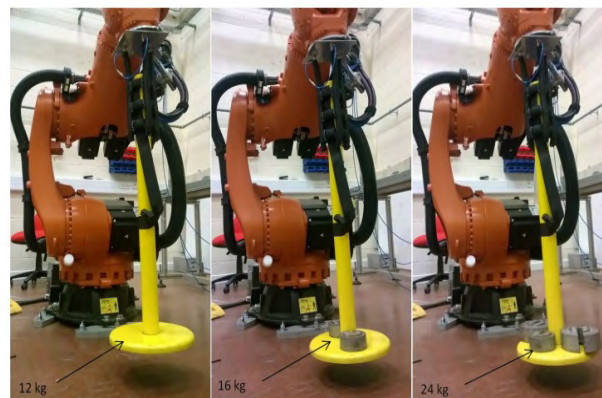


FIGURE 24. The grasping examples for the three CPMA gripper at three different loads.

to 40 kg. A 6 cm diameter of adjustable weight cylindrical object has been used to validate the grasping performances of the extensor-circular gripper of one and three CPMA, respectively. Fig. 23 shows the controller results for both grippers at different object loads. Fig. 24 shows grasping examples of the three CPMA gripper at different loads.

IX. CONCLUSION

Grasping and safe handling of objects is a very important issue in robotic application. The end effector is a part of the robot that has direct contact with the object. Different object dimensions, shapes, materials and weights require different and complex designs of end effectors. The complexity of the design can, in turn, lead to the need for a complex control system.

This article has described the principle of operation and the structure of the pneumatic muscle actuator (PMA). It has explained that the typical use of PMAs is to produce linear motion. However, methods have been explored which allow the actuators to exhibit bending behaviour. A novel bending muscle has been presented based on a single extensor actuator which is reinforced to produce a bending motion; it has also been shown that extensor muscles can be used to create a bending motion if they are formed into a continuum arm consisting of parallel muscles.

A novel bending muscle design, based on a contractor actuator, is presented by inserting a thin incompressible but flexible (2 mm thick) reinforcing rod between the inner tube and the braided sleeve of the muscle to prevent a contraction occurring on one side. This means that when activated, the muscle will cause a bending motion.

The paper then presented two soft gripper designs that use PMAs; a three finger gripper based on a bending contraction PMA and an extension-circular gripper. The physical structure of each gripper is described individually and the grasping performance assessed experimentally.

The first gripper has been shown to provide a wide range of grasping sizes for different object shapes and dimensions and has been demonstrated to have grasp strength sufficient

to hold a 1.4 kg mass. Controlling the air pressure inside the fingers leads to closing of the fingers, the soft nature of the fingers means that they can conform to the shape of the object being grasped without the need for any complex control system or grasp planning.

The extension-circular gripper has two main features; it can extend in length, allowing the main grasping contact area to be appropriately positioned on the object to be grasped. The second feature is a circle shape PMA which, when pressurised, reduces in diameter allowing it to grasp an object placed at its centre. The gripper has been shown experimentally to be capable of lifting loads up to 10.9 kg.

A modification is done to the two grippers to increase their performances and the control system is designed for each gripper to evaluate the design efficiencies.

Future work will concentrate mainly on control of the strategies in terms of the energy used.

## REFERENCES

- G. Fantoni et al., "Grasping devices and methods in automated production processes," *CIRP Ann.*, vol. 63, no. 2, pp. 679–701, 2014.
- N. Wettels, A. R. Parnandi, J.-H. Moon, G. E. Loeb, and G. Sukhatme, "Grip control using biomimetic tactile sensing systems," *IEEE/ASME Trans. Mechatronics*, vol. 14, no. 6, pp. 718–723, Dec. 2009.
- K. B. Shimoga, "Robot grasp synthesis algorithms: A survey," *Int. J. Robot. Res.*, vol. 15, no. 3, pp. 230–266, 1996.
- H. Choi and M. Koç, "Design and feasibility tests of a flexible gripper based on inflatable rubber pockets," *Int. J. Mach. Tools Manuf.*, vol. 46, nos. 12–13, pp. 1350–1361, 2006.
- J. W. S. Martell and G. Gini, "Robotic hands: Design review and proposal of new design process," in *World Academy of Science, Engineering and Technology*, vol. 26, 2007, pp. 85–90.
- T. Hassan, M. Manti, G. Passetti, N. d'Elia, M. Cianchetti, and C. Laschi, "Design and development of a bio-inspired, under-actuated soft gripper," in *Proc. 37th Annu. Int. Conf. IEEE Eng. Med. Biol. Soc. (EMBC)*, Aug. 2015, pp. 3619–3622.
- G. Ratani, M. Cianchetti, G. Ciuti, A. Menciassi, and C. Laschi, "Design and development of a soft robotic gripper for manipulation in minimally invasive surgery: A proof of concept," *Meccanica*, vol. 50, no. 11, pp. 2855–2863, 2015.
- M. E. Giannaccini et al., "A variable compliance, soft gripper," *Auto. Robots*, vol. 36, nos. 1–2, pp. 93–107, 2014.
- R. K. Katschmann, A. D. Marchese, and D. Rus, "Autonomous object manipulation using a soft planar grasping manipulator," *Soft Robot.*, vol. 2, no. 4, pp. 155–164, 2015.
- B. Mosadegh et al., "Pneumatic networks for soft robotics that actuate rapidly," *Adv. Funct. Mater.*, vol. 24, no. 15, pp. 2163–2170, 2014.
- S. Wakimoto, K. Ogura, K. Suzumori, and Y. Nishioka, "Miniature soft hand with curling rubber pneumatic actuators," in *Proc. IEEE Int. Conf. Robot. Autom. (ICRA)*, May 2009, pp. 556–561.
- R. Niiyama, X. Sun, C. Sung, B. An, D. Rus, and S. Kim, "Pouch motors: Printable soft actuators integrated with computational design," *Soft Robot.*, vol. 2, no. 2, pp. 59–70, 2015.
- A. Stilli, H. A. Wurdemann, and K. Althoefer, "Shrinkable, stiffness-controllable soft manipulator based on a bio-inspired antagonistic actuation principle," in *Proc. IEEE/RSJ Int. Conf. Intell. Robots Syst. (IROS)*, Sep. 2014, pp. 2476–2481.
- F. Maghooa, A. Stilli, Y. Noh, K. Althoefer, and H. A. Wurdemann, "Tendon and pressure actuation for a bio-inspired manipulator based on an antagonistic principle," in *Proc. IEEE Int. Conf. Robot. Autom. (ICRA)*, May 2015, pp. 2556–2561.
- L. A. Al Abeach, S. Nefti-Meziani, and S. Davis, "Design of a variable stiffness soft dexterous gripper," *Soft Robot.*, vol. 4, no. 3, pp. 274–284, 2017.
- R. Deimel and O. Brock, "A compliant hand based on a novel pneumatic actuator," in *Proc. IEEE Int. Conf. Robot. Autom. (ICRA)*, May 2013, pp. 2047–2053.
- F. Ilievski, A. D. Mazzeo, R. F. Shepherd, X. Chen, and G. M. Whitesides, "Soft robotics for chemists," *Angew. Chem.*, vol. 123, no. 8, pp. 1930–1935, 2011.
- R. Deimel and O. Brock, "A novel type of compliant and underactuated robotic hand for dexterous grasping," *Int. J. Robot. Res.*, vol. 35, nos. 1–3, pp. 161–185, 2016.
- B. S. Homberg, R. K. Katschmann, M. R. Dogar, and D. Rus, "Haptic identification of objects using a modular soft robotic gripper," in *Proc. IEEE/RSJ Int. Conf. Intell. Robots Syst. (IROS)*, Sep/Oct. 2015, pp. 1698–1705.
- J. Amend, N. Cheng, S. Fakhouri, and B. Culley, "Soft robotics commercialization: Jamming grippers from research to product," *Soft Robot.*, vol. 3, no. 4, pp. 213–222, 2016.
- B. Wang, K. C. Aw, M. Biglari-Abhari, and A. McDaid, "Design and fabrication of a fiber-reinforced pneumatic bending actuator," in *Proc. IEEE Int. Conf. Adv. Intell. Mechatronics (AIM)*, Jul. 2016, pp. 83–88.
- I. N. A. M. Nordin, M. R. M. Razif, E. Natarajan, K. Iwata, and K. Suzumori, "3-D finite-element analysis of fiber-reinforced soft bending actuator for finger flexion," in *Proc. IEEE/ASME Int. Conf. Adv. Intell. Mechatronics (AIM)*, Jul. 2013, pp. 128–133.
- A. A. M. Faudzi, M. R. M. Razif, I. N. A. M. Nordin, K. Suzumori, S. Wakimoto, and D. Hirooka, "Development of bending soft actuator with different braided angles," in *Proc. IEEE/ASME Int. Conf. Adv. Intell. Mechatronics (AIM)*, Jul. 2012, pp. 1093–1098.
- B. Wang, A. McDaid, T. Giffney, M. Biglari-Abhari, and K. C. Aw, "Design, modelling and simulation of soft grippers using new bimorph pneumatic bending actuators," *Cogent Eng.*, vol. 4, no. 1, 2017, Art. no. 1285482.
- J. Guo, K. Elgeneidy, C. Xiang, N. Lohse, L. Justham, and J. Rossiter, "Soft pneumatic grippers embedded with stretchable electroadhesion," *Smart Mater. Struct.*, vol. 27, no. 5, p. 055006, 2018.
- J. Shintake, S. Rosset, B. Schubert, D. Floreano, and H. Shea, "Versatile soft grippers with intrinsic electroadhesion based on multifunctional polymer actuators," *Adv. Mater.*, vol. 28, no. 2, pp. 231–238, 2016.
- M. R. M. Razif, M. Bavandi, I. N. A. M. Nordin, E. Natarajan, and O. Yaakob, "Two chambers soft actuator realizing robotic gymnotiform swimmers fin," in *Proc. IEEE Int. Conf. Robot. Biomimetics (ROBIO)*, Dec. 2014, pp. 15–20.
- M. R. M. Razif et al., "Non-linear finite element analysis of biologically inspired robotic fin actuated by soft actuators," *Appl. Mech. Mater.*, vol. 528, pp. 272–277, Feb. 2014.
- E. Natarajan et al., "Numerical dynamic analysis of a single link soft robot finger," *Appl. Mech. Mater.*, vol. 459, pp. 449–454, Oct. 2014.
- S. Davis, N. Tsagarakis, J. Canderle, and D. G. Caldwell, "Enhanced modelling and performance in braided pneumatic muscle actuators," *Int. J. Robot. Res.*, vol. 22, nos. 3–4, pp. 213–227, 2003.
- J. S. Tate, A. D. Kelkar, and J. D. Whitcomb, "Effect of braid angle on fatigue performance of biaxial braided composites," *Int. J. Fatigue*, vol. 28, no. 10, pp. 1239–1247, 2006.
- W. Liu and C. R. Rahn, "Fiber-reinforced membrane models of McKibben actuators," *J. Appl. Mech.*, vol. 70, no. 6, pp. 853–859, 2003.
- J. Sárosi, I. Bíró, J. Németh, and L. Cveticanin, "Dynamic modeling of a pneumatic muscle actuator with two-direction motion," *Mech. Mach. Theory*, vol. 85, pp. 25–34, Mar. 2015.
- A. Al-Ibadi, S. Nefti-Meziani, and S. Davis, "Efficient structure-based models for the McKibben contraction pneumatic muscle actuator: The full description of the behaviour of the contraction PMA," *Actuators*, vol. 6, no. 4, p. 32, 2017.
- A. Al-Ibadi, S. Nefti-Meziani, and S. Davis, "Valuable experimental model of contraction pneumatic muscle actuator," in *Proc. 21st IEEE Int. Conf. Methods Models Autom. Robot. (MMAR)*, Miedzyzdroje, Poland, Aug./Sep. 2016, pp. 744–749.
- W. McMahan et al., "Field trials and testing of the OctArm continuum manipulator," in *Proc. IEEE Int. Conf. Robot. Autom. (ICRA)*, May 2006, pp. 2336–2341.
- A. Al-Ibadi, S. Nefti-Meziani, and S. Davis, "Novel models for the extension pneumatic muscle actuator performances," in *Proc. 23rd Int. Conf. Autom. Comput. (ICAC)*, Sep. 2017, pp. 1–6.
- G. Andrikopoulos, G. Nikolakopoulos, and S. Manesis, "Advanced nonlinear PID-based antagonistic control for pneumatic muscle actuators," *IEEE Trans. Ind. Electron.*, vol. 61, no. 12, pp. 6926–6937, Dec. 2014.
- C. W. Goodmurphy and W. K. Ovalle, "Morphological study of two human facial muscles: Orbicularis oculi and corrugator supercilii," *Clin. Anatomy*, vol. 12, no. 1, pp. 1–11, 1999.



robotics, pneumatic muscle actuators, multi-robot systems, and intelligent control.

**ALAA AL-IBADI** received the bachelor's degree in electrical engineering and the M.Sc. degree in computer and control system from the University of Basrah, Iraq, in 2001 and 2005, respectively. He is currently pursuing the Ph.D. degree with the University of Salford, Manchester, U.K. He was an Assistant Lecturer with the Computer Engineering Department, University of Basrah. His research interests include biologically inspired systems, soft



Network SMART-E and the coordinator and co-I of three further major national programs worth over 14 million. She is a member of the Advisory Board of the U.K. Research Council—EPSRC. She is one of the founding members of the Northern Robotics and Autonomous Systems Network which is part of the Innovate U.K. Network. She serves on the Advisory Board of the EPSRC National Centre in Innovative Manufacturing. She is the Vice Chairman of the IEEE Robotics and Automation UK & RI. She is an Associate Editor of the IEEE TRANSACTIONS ON FUZZY SYSTEMS.

**SAMIA NEFTI-MEZIANI** received the Ingeniorat d'etat and DEA degrees in industrial engineering and the Ph.D. degree in robotics. She is currently the Chair in Robotics and the Director of the Centre for Autonomous Systems and Advanced Robotics, University of Salford. She has a well-established track record and has published extensively in the areas of advanced robotics and autonomous systems. She is the Coordinator of the European Marie Curie Innovative Training



research funding, most notably the Euro 3 948 470 Marie Curie Initial Training Networks and Sustainable Manufacturing through Advanced Robotics Training in Europe. He has published extensively and has also co-authored chapters in two books on automation. His research interests include actuators, biologically inspired systems, biomimetics, soft robotics, humanoid robots, end-effectors and dexterous hands, and industrial automation, particularly in the food industry. He has been an associate editor at several IEEE conferences. He is a Guest Editor of a special edition of the journal *Actuators*.

• • •